Corrosion Science 75 (2013) 58–66

Contents lists available at SciVerse ScienceDirect

Corrosion Science

journal homepage: www.elsevier.com/locate/corsci

Chromia layer growth on a Ni-based superalloy: Sub-parabolic kinetics and the role of titanium

S. Cruchley [a], H.E. Evans [a,*], M.P. Taylor [a], M.C. Hardy [b], S. Stekovic [c,1]

[a] School of Metallurgy and Materials, The University of Birmingham, B15 2TT Birmingham, UK
[b] Rolls-Royce plc, Elton Road, DE24 8BJ Derby, UK
[c] Linköping University, 581 83 Linköping, Sweden

ARTICLE INFO

Article history:
Received 17 March 2013
Accepted 21 May 2013
Available online 7 June 2013

Keywords:
A. Superalloys
C. Oxidation
C. Selective Oxidation

ABSTRACT

Oxidation of the Ni-based superalloy RR1000 has been undertaken in air over the temperature range 600–900 °C for times up to 5000 h. The surface oxide consisted of a protective Ti-doped chromia layer but with rutile forming on its outer surface. Sub-surface oxidation of Al and Ti also occurred. The thickening kinetics of the chromia layer were sub-parabolic with initial rates around two orders of magnitude higher than expected for Ti-free chromia. This enhancement and the sub-parabolic kinetics are accounted for by Ti-doping of the chromia layer. Over time the enhancement reduced because of Ti-depletion in the alloy.

1. Introduction

Nickel-based superalloys have been optimised, compositionally and microstructurally, to operate in the highly stressed conditions occurring in the hot sections of aero- or land-based gas turbine engines. The high temperatures experienced by components in these operating conditions have implications on the performance of the alloys used. Under such conditions degradation by oxidation occurs and plays a key role in determining the lifetimes of the components. One method of improving the efficiency of these engines is by increasing the operating temperatures. This will inevitably result in accelerated degradation of the alloys. For this reason it is important to understand the oxidation processes occurring and the mechanisms involved.

Superalloys used for turbine discs have operating temperatures typically $\leqslant$700 °C and form a continuous layer of chromia rather than alumina [1–5] under these conditions. This layer is often protective in that the oxygen potential beneath it is sufficient to oxidise only aluminium and titanium, of the major alloy constituents [1,3,5]. Oxides of these elements form internal, sub-surface particles, often as acicular intergranular penetrations. In addition, Ti-rich oxides are known to form on the outer surface of the chromia layer [1,3,5]. Oxidation studies on such Ni-based alloys have tended to use weight-change measurements to assess the reaction kinetics and have shown that the rate of oxidation is higher than would be anticipated for protective chromia formation [5]. This, of course, is not unexpected given that other alloy constituents (Ti and Al, in particular) are also being oxidised. It remains unclear, however, whether the chromia layer itself thickens at rates commensurate with those found on simpler alloys and pure chromium or whether the complex compositions of Ni-based alloys can lead to doping effects that produce a systematic difference in chromia growth rates. The purpose of this present work is to assess this possibility through detailed metallography of long-term oxidation specimens of the RR1000 Ni-based superalloy.

2. Experimental procedure

The RR1000 alloy used in this study was produced using a powder metallurgy route followed by a heat treatment to obtain a grain size of between 30 and 50 μm. The alloy has a two-phase microstructure consisting of a γ (nominally Ni,Co) matrix and approximately a 45% volume fraction of γ' precipitates (nominally $Ni_3[Al,Ti]$). The nominal composition of the alloy was: Ni 52.3, Co 18.5, Cr 15.0, Mo 5.0, Ti 3.6, Al 3.0, Ta 2.0, Hf 0.5, Zr 0.06, C 0.027, B 0.015 wt%. This was confirmed for all elements except carbon, boron and zirconium during the course of this study using Energy Dispersion Spectroscopy (EDS).

Oxidation testing was conducted over the temperature range of 600–900 °C in laboratory air for times up to 5000 h. The size of the specimens used was approximately 20 mm by 10 mm by 2 to 5 mm thick. The specimens were cut to size using electro-discharge machining (EDM) and all the surfaces were ground on

---

* Corresponding author. Tel.: +44 (0) 121 414 5172.
E-mail addresses: SXC697@adf.bham.ac.uk (S. Cruchley), h.e.evans@bham.ac.uk (H.E. Evans), m.p.taylor@bham.ac.uk (M.P. Taylor), Mark.Hardy@rolls-royce.com (M.C. Hardy), svjetlana.stekovic@liu.se (S. Stekovic).

[1] Formerly, Rolls-Royce plc.

0010-938X/$ - see front matter © 2013 Elsevier Ltd. All rights reserved.
http://dx.doi.org/10.1016/j.corsci.2013.05.016

Table 1
Test matrix showing (√) exposure times at which specimens were removed for examination. Tests marked with an * were performed using TGA rigs. The remainder of the tests were performed in static furnaces. All tests were performed in laboratory air.

Time (h) Temp. (°C)	24	50	100	300	500	1000	2000	5000
600 °C						√		
650 °C				√*				
700 °C	√	√	√*	√	√	√	√	√
750 °C	√	√	√*	√	√	√	√	
800 °C	√	√	√*	√	√	√	√	
850 °C			√*					
900 °C			√*					

wet SiC paper and polished using 6 μm diamond paste to remove the damage from the EDM process and to produce a surface finish, R_a, of approximately 0.4 μm. All edges and corners were chamfered to reduce stress concentrators and polished to the same surface finish. The final dimensions after polishing were measured using a micrometer and the surface area calculated. Following this, the specimens were cleaned in ethanol, dried and weighed on a five figure calibrated balance.

The results from two types of oxidation test are combined in this study. Table 1 shows the test matrix with the two approaches included. All the 100 h tests and the test conducted at 650 °C were performed using a thermogravimetric balance (TGA). The weight change during these tests was monitored continually and adjusted to accommodate buoyancy effects. All other tests were conducted in horizontal tube furnaces. For these latter tests, batches of specimens were placed in alumina boats and inserted into the furnaces at temperature. Intermittent weighing at room temperature was used to determine the oxidation kinetics. At selected time intervals, a specimen was removed from the batch for examination before the high temperature exposure continued for the remainder of the batch. Table 1 shows the time intervals chosen for examination. At 600 °C one isothermal test, having an exposure time of 1000 h, has been performed to date.

After oxidation testing and re-weighing, the surfaces of the specimens were sputter coated with gold and examined by scanning electron microscopy (SEM) using both secondary (SE) and backscattered electrons (BSE). Following this, the specimens were nickel-plated and mounted in resin or vacuum impregnated in a low viscosity resin. The specimens were prepared for cross-sectional analysis by grinding on SiC papers down to 1200 grit using water as a lubricant followed by polishing using progressively finer diamond paste from 6 μm down to 0.25 μm. The cross-sections were examined using a high resolution JEOL 7000F FEGSEM. This equipment is fitted with wave-length dispersive spectroscopy (WDS), used here for the identification of oxygen and nitrogen, and EDS used for heavier element compositional identification, mapping and line scans. X-ray diffraction (XRD) analysis of the surface oxides was performed on a Philips XPert system using Cu Kα radiation, indexed between a 2θ of 10–100°.

3. Results and discussion

3.1. Gravimetric oxidation kinetics

Fig. 1 shows the change in specimen weight with time over the temperature range tested. No spallation was observed for any of the specimens tested. These weight gain data were plotted (Fig. 2) according to Eq. (1) to obtain the best-fit values of 'n', given in Table 2.

$$(\Delta m)^n = k'_n t \tag{1}$$

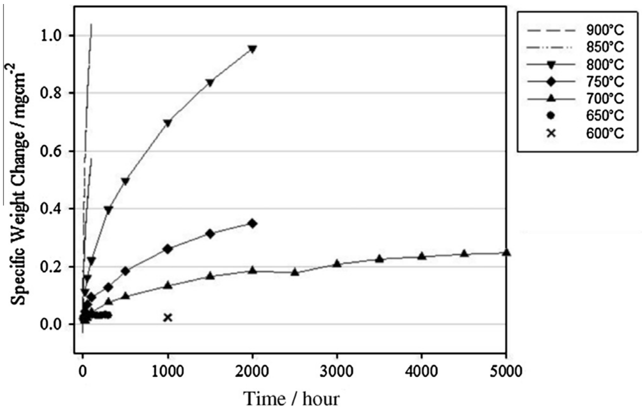

Fig. 1. Plot of specific weight change against time for each temperature. The data at 650, 850 and 900 °C were obtained from TGA tests, at the other temperatures the data were obtained by weighing batches of samples at 500 h interval.

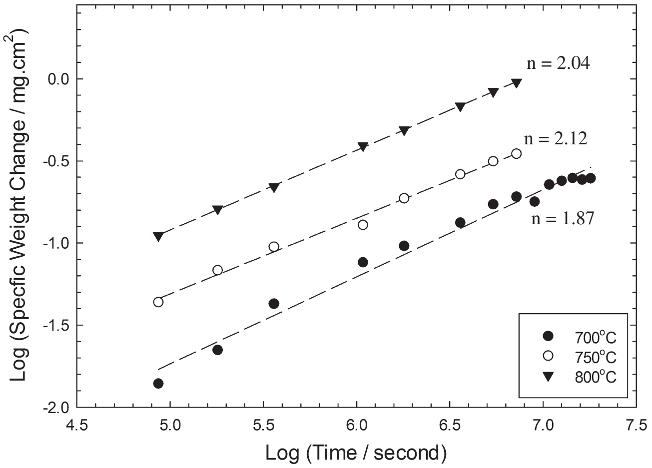

Fig. 2. Plot of log specific weight change against log exposure time for 700 °C, 750 °C and 800 °C showing that the weight gain kinetics can be approximated to parabolic behaviour, $n = 2$ (Eq. (1)).

Table 2
Best-estimate values of the exponent, n, (Eq. (1)) for weight gain kinetics and maximum exposure time at each temperature; n.d. – not determined.

Temperature (°C)	n	Maximum exposure time (h)
900	2.2	100
850	2.2	100
800	2.04	2000
750	2.12	2000
700	1.87	5000
650	n.d.	350
600	n.d.	1000

Here (Δm) is the specific weight gain in mg cm^{-2}, t is exposure time in seconds and k'_n is a rate constant. It can be appreciated from Table 2 that the values of n, at least at the highest temperatures, are sufficiently close to 2 that parabolic kinetics can be assumed, i.e. $n = 2$ in Eq. (1) and $k'_n = k'_p$, the parabolic rate constant expressed in terms of weight gain. It was assumed that parabolic conditions also obtained for the two lowest temperatures used although the data were limited at these temperatures. The parabolic rate constants calculated from Eq. (1) for all temperatures used in the present work are shown in the second column of Table 3. Also shown in Table 3, in the third column, are the parabolic rate constants determined from relatively short-term (100 h) tests,